Nat. Hazards Earth Syst. Sci., 12, 327–340, 2012
www.nat-hazards-earth-syst-sci.net/12/327/2012/
doi:10.5194/nhess-12-327-2012

Natural Hazards and Earth System Sciences

Factors selection in landslide susceptibility modelling on large scale following the gis matrix method: application to the river Beiro basin (Spain)

D. Costanzo[1], E. Rotigliano[1], C. Irigaray[2], J. D. Jiménez-Perálvarez[2], and J. Chacón[2]

[1]Department of Earth and Sea Sciences, University of Palermo, Italy
[2]Department of Civil Engineering, ETSICCP, University of Granada, Spain

Correspondence to: D. Costanzo (costanzodario@gmail.com)

Received: 3 April 2011 – Revised: 27 December 2011 – Accepted: 4 January 2012 – Published: 13 February 2012

Abstract. A procedure to select the controlling factors connected to the slope instability has been defined. It allowed us to assess the landslide susceptibility in the Rio Beiro basin (about 10 km^2) over the northeastern area of the city of Granada (Spain). Field and remote (Google EarthTM) recognition techniques allowed us to generate a landslide inventory consisting in 127 phenomena. To discriminate between stable and unstable conditions, a diagnostic area had been chosen as the one limited to the crown and the toe of the scarp of the landslide. 15 controlling or determining factors have been defined considering topographic, geologic, geomorphologic and pedologic available data. Univariate tests, using both association coefficients and validation results of single-variable susceptibility models, allowed us to select the best predictors, which were combined for the unique conditions analysis. For each of the five recognised landslide typologies, susceptibility maps for the best models were prepared. In order to verify both the goodness of fit and the prediction skill of the susceptibility models, two different validation procedures were applied and compared. Both procedures are based on a random partition of the landslide archive for producing a test and a training subset. The first method is based on the analysis of the shape of the success and prediction rate curves, which are quantitatively analysed exploiting two morphometric indexes. The second method is based on the analysis of the degree of fit, by considering the relative error between the intersected target landslides by each of the different susceptibility classes in which the study area was partitioned. Both the validation procedures confirmed a very good predictive performance of the susceptibility models and of the actual procedure followed to select the controlling factors.

1 Introduction

One of the key points in assessing landslide susceptibility by means of multivariate statistical models is the selection of the controlling factors (i.e., the predictor variables). Particularly when adopting approaches based on conditional analysis, such as UCU or Matrix methods, increasing the number of factors is the reason for a higher number of combinations and a consequent decreasing of the number of cases (counts of cells) for which each specific condition is observed and "trained". At the same time procedures for forward selection or backward elimination are not available for such landslide density based methods. Procedures and criteria for classifying the importance of each of the considered factors and a priori taking a decision whether to include a single factor in the definition of multivariate models are needed. Among the possible approaches, the statistical analysis of contingency tables produced by spatially crossing factors and landslides allows for the computing of some correlation or association indexes, capable of driving the decision (Fernández et al., 2003; Chacón et al., 2006; Irigaray et al., 2007; Jiménez-Perálvarez et al., 2009). Parametric and non-parametric statistical methods are widely adopted in deriving association, co-graduation and correlation indexes that express the strength and significance with which a predictor variable explains the outcome (stable/unstable conditions). But, to exhaustively define a procedure for the best factors selection, evaluations are also required on the predictive performances both for each single-variable model and for the multivariate models, which are obtained by variously selecting these. In fact, the results of the validation procedures are also controlled by the spatial stability of such geostatistical relationships, when splitting in *training* and *test* sub-sets

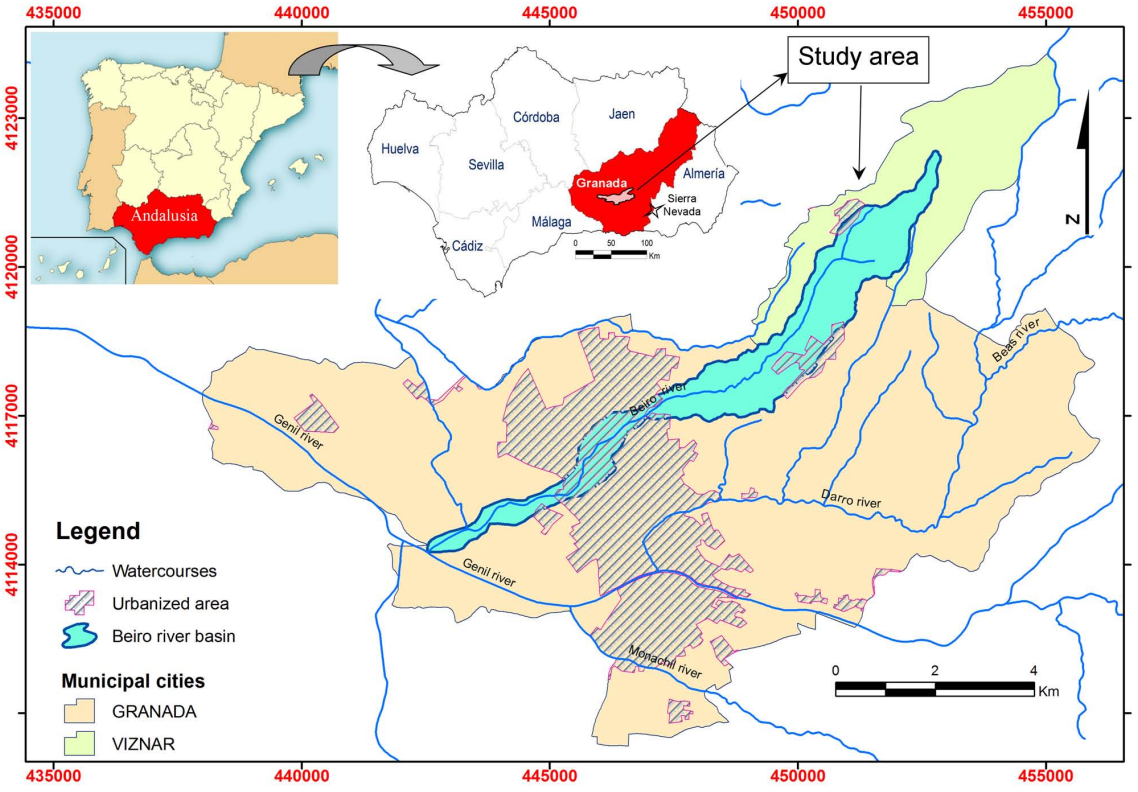

Fig. 1. Geographical setting of the study zone. Coordinate Reference System: UTM zone 30 European Datum 50.

UCUs or landslides. In the present paper, results are presented of a research aimed at analysing the relationships between a priori ranking of controlling factors and predictive performance of multivariate models prepared by singling out the best ones to be combined.

2 Materials and methods

2.1 Setting of the study area

The study area (Fig. 1) stretches NE of the city of Granada (Andalusia, Spain), coinciding with the basin of the Beiro river (10 km^2), which is a sub-basin of the Genil river, a subsidiary of the Guadalquivir river that flows through the south of Spain to the Atlantic Ocean. Despite the nearness to the sea, the climate in the area is Mediterranean with a continental influence, being characterised by marked temperature and rainfall short- and long-period changes. According to the termo-pluviometric station of "Granada-Cartuja", 720 m a.s.l., rainfall is mainly concentrated between October and April, while between May and September it is generally very low (particularly in July and August when it is less than 10 mm). It rarely rains and the high mountains of Sierra Nevada do not allow the sea to mitigate the climate. Temperatures in winter are often below zero while in summer they are always above 30 °C. High diurnal temperature ranging is also recorded, reaching up to 15 °C. According to the De Martonne aridity index (1942) the area can be classified as a semi-arid climate.

The geological setting of the Beiro river basin (Fig. 2) is characterised by terrains, which are aged from Pliocene to recent Quaternary, being tectonically limited to the North by Triassic dolomitic marbles which are very tectonised (Vera, 2004). This terrain is the only formation of the Alpujarride complex that outcrops into the study zone. This complex is followed by Pliocene deposits and incoherent Pleistocene and Quaternary post-orogenic deposits that filled deep valleys, producing the great alluvial fans. The post-orogenic deposits which outcrop into the study zone, from bottom to top, are: the terrains of the "Pinos-genil formation", that marks the transition to continental facies (mainly Pliocenic conglomerates and, in the higher part of the sequence, sandy layers); the Cenes-Jun sequence, made of lacustrine deposits of lutite, sand, silt and gravel; the "Alhambra conglomerates" sequence made mainly of conglomerates and sand. The sequence is closed by Quaternary alluvial deposits which are the terrain on which the town is settled.

The landscape is generally marked by sub-planar areas, corresponding to a lower Pleistocene smoothing of the previous relief deeply engraved by Upper Pleistocene to Holocene stream incision, surrounded by steep reliefs. The

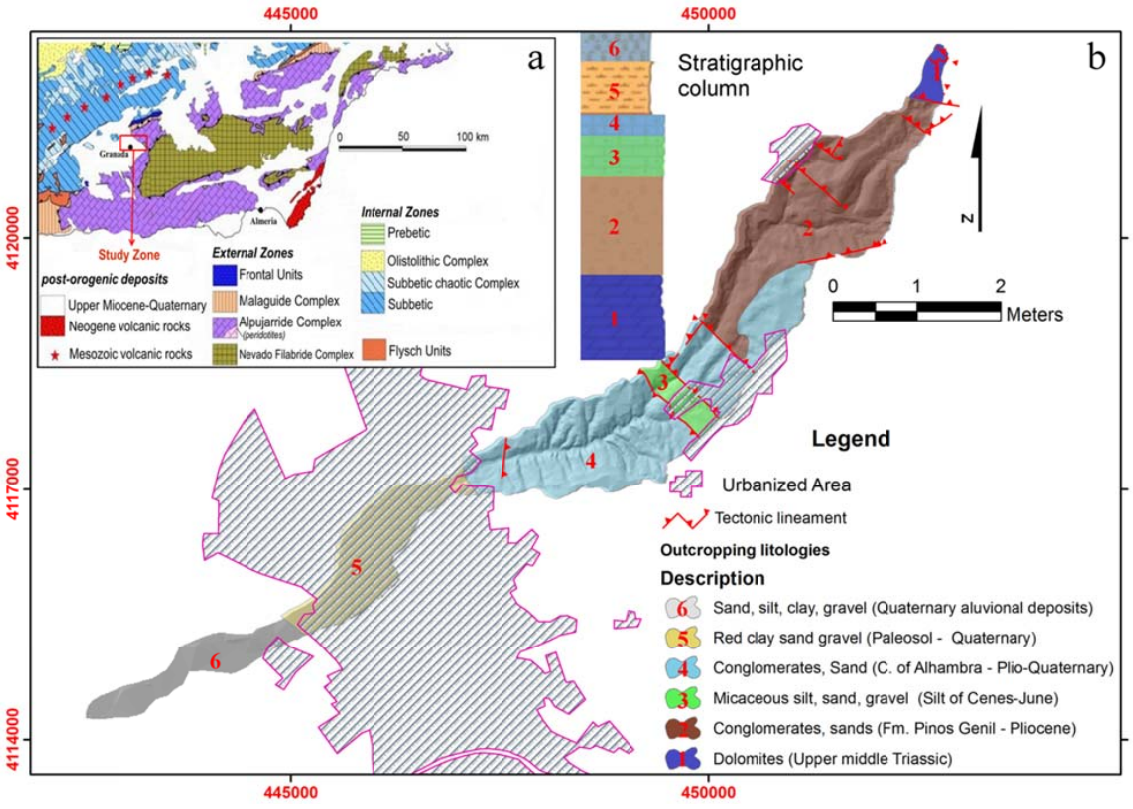

Fig. 2. Geological setting of the study zone. Regional geology **(a)** (modified from Vera, 2004); Beiro river basin **(b)**. Coordinate Reference System: UTM zone 30 European Datum 50.

geomorphological setting, together with the climatic conditions, is responsible for a wide diffusion of landslides, characterised by several movement typologies and variable area extensions (Chacón et al., 2006)

2.2 Landslides

A database of 127 slope movements (Fig. 3) has been produced for the Beiro river basin, the movements have been classified (Varnes, 1978; Cruden and Varnes 1996, Dikau et al., 1996) as falls, translational slides, earth flows, debris flows and flow slides (Table 1). The archive was obtained by using different recognition techniques. First, we analysed and interpreted the aerial photos in a scale of 1:33 000 taken between 1956–1957 by "Ejército del Aire de España" and the European air force (also known as "the American flight") and the ones taken in scale of 1:18.000 by the Geographic Minerary Institute of Spain (IGME) in 1978. Another step towards the definition of the landslide archive was a field survey carried out in scale of 1:10 000 between March and April 2010. During the field survey, rock and soil samples were collected and analysed, in order to distinguish between debris and earth type material. The landslide archive obtained was compared to the one obtained through the use of open source software or free images like Google Earth (GE) and similar (e.g., Bing Maps 3-D, aerial photos, etc.) (see also Conoscenti et al., 2009; Costanzo et al., 2011; Rotigliano et al., 2011b). The latter were chosen because of the excellent spatial resolution (DigitalGlobe Catalog ID: 1010010007D4E108, Acquisition Date: 24 March 2008; Catalog ID: 1010010004736A01, Acquisition Date: 15 August 2005; spatial resolution 46–60 cm per pixel) of the images, as well as their easy access to updated cartography and of the possibility to dynamically manage the angles for each slope (Fig. 4).

The landslide survey has enabled an archive to be prepared:

– Falls (28 cases, 3.8 % of the landslide area): these landslides mainly affect the over-consolidated silty and sandy quaternary terrains. The fall movements found in this area are not very extended and cover areas of tens of square metres each. The areas affected by this kind of movement are usually the ones where the geostructural conditions form near vertical slopes. Weathering processes, a high diurnal and seasonal temperature ranging, are responsible for fractures enlargement inside over-consolidated soils. The triggering factors for fall movements are the undercutting at the foot of escarpments and the intensive rainfall.

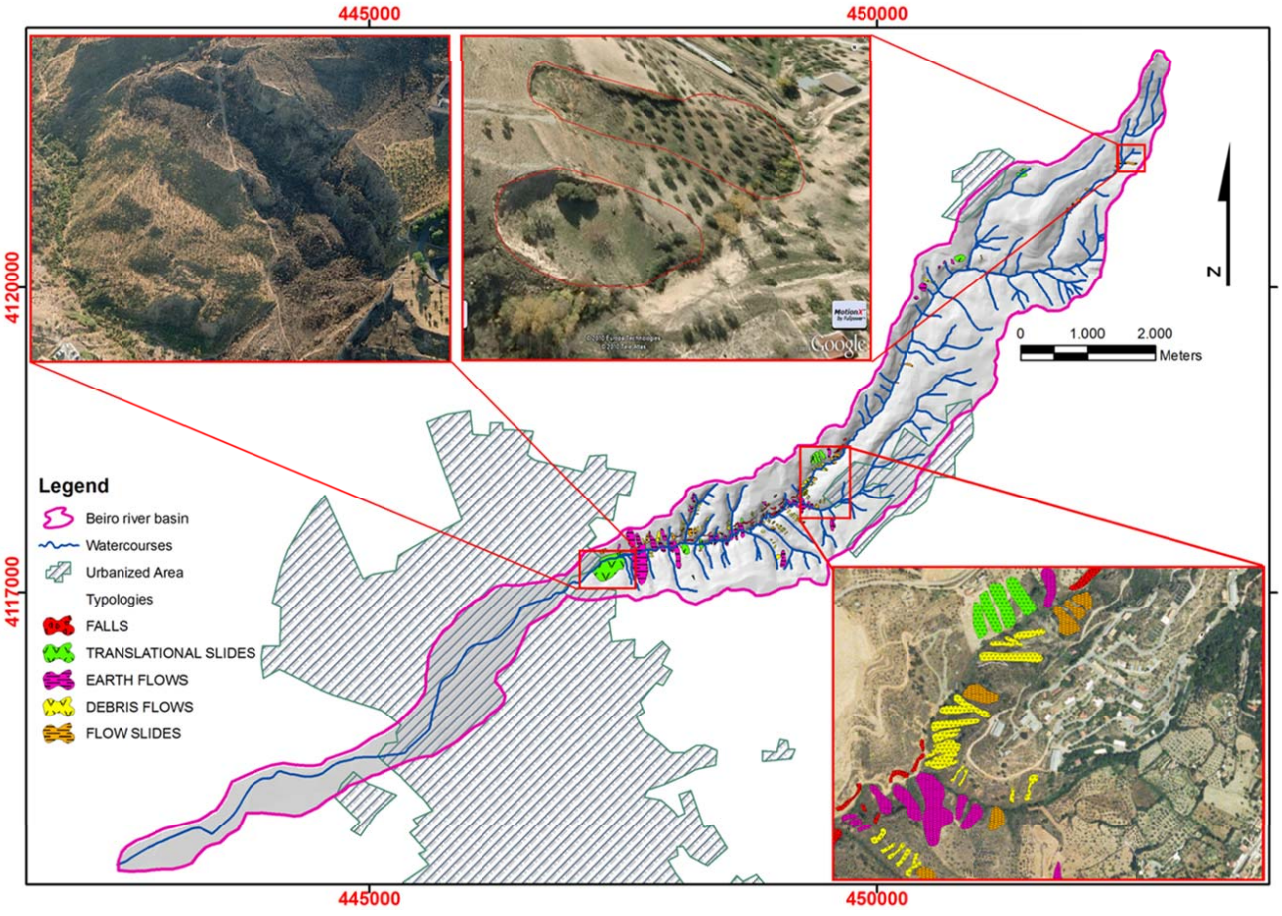

Fig. 3. Landslide inventory. Spatial distribution of landslide, obtained for the Beiro river basin by Google EarthTM remote analysis. Coordinate Reference System: UTM zone 30 European Datum 50.

Table 1. Landslide inventory, extension of landslide and lithology affected by slope ruptures.

TYPOLOGY	number of cases	area (m^2) for a single landslide					Percentages		Affected lithology (% of cases)					
		max	min	mean	total	Std. Dev.	T1	T2	Al	Rcsg	SoCJ	Alh	Cs	Dol
Falls	28	1802	50	356	14 249	390.1	3.8	0.1	0.0	0.0	15.2	75.1	9.7	0.0
Translational slides	1	69 755	69 755	69 755	69 755	–	18.7	0.7	0.0	0.0	0.0	100	0.0	0.0
Earth flows	36	48 997	165	3668	201 788	6704.3	54.2	2.1	0.0	0.0	5.2	60.2	34.6	0.0
Debris flows	57	2984	85	571	47 438	526.0	12.7	0.5	0.0	0.0	13.2	65.4	21.4	0.0
Flow-slides	5	9758	434	2204	39 683	2108.6	10.6	0.4	0.0	0.0	17.1	67.3	15.6	0.0
Total	127				372 913		100.0	3.81 %	Area of Beiro river basin 9.8 km^2					

Al: Aluvional deposits. Rcsg: red clay, sand and gravel. Alh: Conglomerates of Alhambra. SoCJ: Silt of Cenes-June. Dol: dolomites. T1: percentage in terms of landslide area. T2: percentage in terms of total area. Std. Dev: standard deviation.

– Translational slide (1 case, 18.7 % of the landslide area): a single landslide, which is locally called the Beiro's translational slide, affecting conglomeratic deposits with sandy and silty intercalations (Alhambra Formation). The extension of the movement reaches up to 70 000 m^2 with a main body 420 m wide and 225 m long. The movement is characterised by a diachronic activity, alternating dormant to active stage, with low or extremely low velocity (Chacón, 2008a, b; 2010; Chacón et al., 2010).

– Earth flows (36 cases, 54.2 % of the landslide area): the terrains interested by earth flows are over-consolidated sands and silts, or conglomerates.

– Debris flows (57 cases, 12.7 % of the landslide area): these are the most common slope failures in the

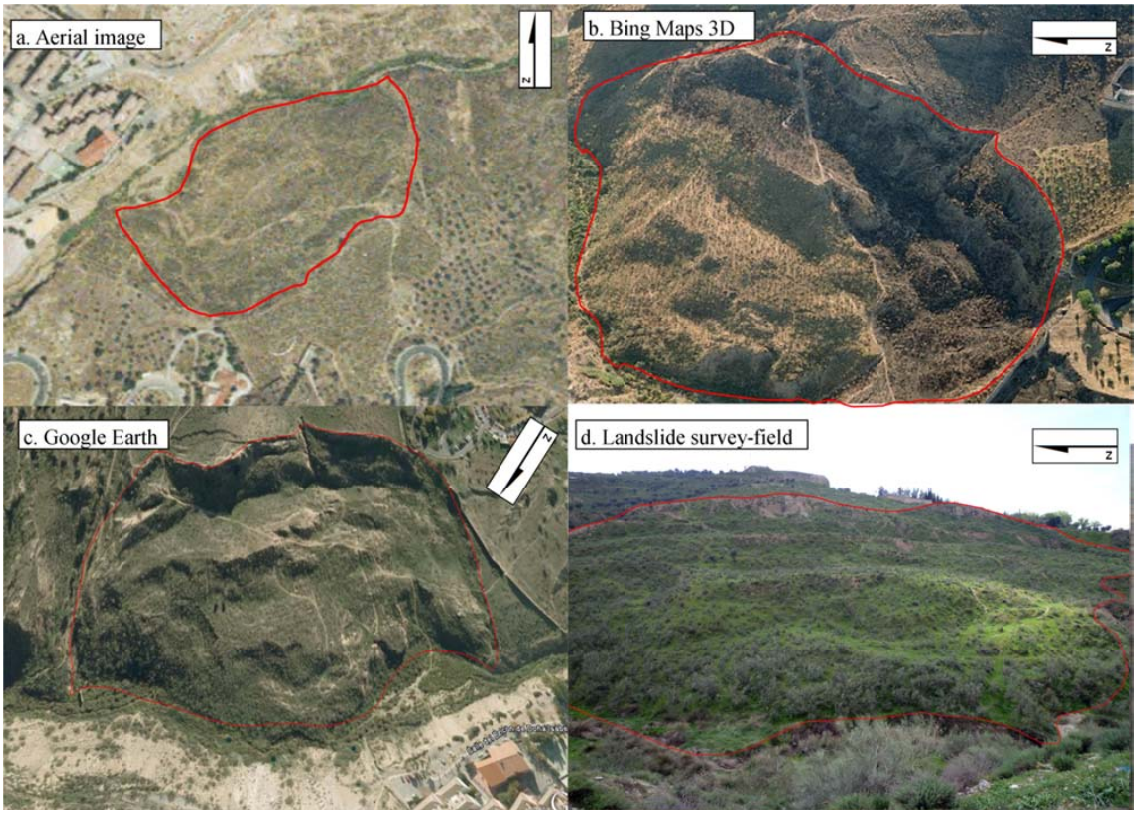

Fig. 4. Beiro translational slide view by different techniques.

area, but they only cover 0.5 % of the Beiro river basin. The debris flows involve terrains mainly consisting of surficial regolithic layers produced by intensive weathering and typically occur, triggered by rainfall, along highly steep slopes.

– Flow-slides (5 cases, 10.6 % of the landslide area): these landslides (representing the 10.6 % of the total landslide area) are complex movements that initiate with the structural collapsing and the flowing of saturated earth or debris volumes, the movement of the mass evolves downhill in a lobate accumulation area (Dikau et al., 1996). The terrains typically interested by flow-slides are carbonates, sandstones and conglomerates. The slip surface is not easily defined for this type of landslide.

In Sect. 1, the discovery of America was described. Here we will outline the subsequent history until the present. This is best summarized in Table 1.

As can be seen from Table 1, there is almost no mention of geomagnetism or the magnetosphere at all. This sorry situation is discussed further and explained away in Sect. 4.

2.3 Susceptibility modelling

In order to define the landslide susceptibility in the Beiro river basin, the matrix method in a GIS environment was applied (Irigaray et al., 1999; Irigaray et al., 2007; Jiménez-Perálvarez, 2009). This approach is based on the determination of all the possible combinations, between the multivariate mapping units, the ones to be classified according to a susceptibility scale, and of the diagnostic areas, which are derived from landslide inventories and allow us to discriminate between stable and unstable conditions. The susceptibility of each mapping unit is defined as a function of its conditioning factors, depending on the spatial relationships between factors and past landslides. The susceptibility level of each UCU is computed as the ratio between unstable and total areas according to the landslide-susceptibility matrix values (LMS) that constitute the proportion of slope movements with respect to the total area and represent the relative susceptibility of each combination of factors at each point of the terrain. A very similar theoretical background has been used by different authors (Davis, 1973; Carrara et al., 1991, 1995; Soeters and van Westen, 1996; Guzzetti et al., 1999, 2006; Clerici et al., 2002; Chung and Fabbri, 2003; Conoscenti et al., 2008).

According to largely adopted procedures (e.g., Fernández et al., 2003; Rotigliano et al., 2011b), the landslide scarp or source area has been used as the diagnostic area, as it better allows to single out physical-environmental conditions that are similar to those responsible for the past landslide activations. According to Fernández (2003), we will refer to this area as “rupture zone”.

Table 2. Correlation between the source area of the landslide and the determining factors. Factors highlighted in grey show the best models.

(A) Falls					(B) Translational slides					(C) Earth flows				
FACTOR	*R*	G-K	ARPA	SHIFT	FACTOR	*R*	G-K	ARPA	SHIFT	FACTOR	*R*	G-K	ARPA	SHIFT
ROUGH	0.48	0.97	0.467	0.00	USE	0.54	−0.72	−0.243	0.61	USE	0.54	−0.73	0.393	−0.11
USE	0.47	0.96	0.453	0.00	TWI	0.44	−0.63	0.172	0.08	SLOPE	0.43	0.67	0.266	0.03
SLOPE	0.42	0.95	0.450	0.02	SLOPE	0.44	−0.62	0.028	−0.18	LITH	0.52	−0.67	0.350	−0.02
EDAF	0.28	−0.68	0.376	0.01	DIST	0.43	0.55	0.112	0.08	ROUGH	0.16	0.67	0.254	0.01
SPI	0.20	0.48	0.248	0.05	ILL	0.42	0.54	0.291	−0.07	TWI	0.36	−0.67	0.275	0.04
TWI	0.20	−0.41	0.177	0.04	GEOM	0.31	0.48	−0.047	0.40	ELEV	0.27	0.67	0.378	−0.09
LITH	0.19	−0.41	0.022	−0.30	ROUGH	0.31	0.47	0.083	0.09	SPI	0.17	0.29	0.084	0.01
ELEV	0.32	−0.38	0.353	0.06	LITH	0.40	0.45	0.137	0.20	GEOM	0.46	−0.21	0.324	0.01
DIST	0.14	−0.34	0.235	0.04	ASPECT	0.39	0.44	0.170	0.18	DIST	0.28	0.25	−0.141	0.31
ILL	0.50	−0.29	0.221	0.14	SPI	0.25	0.33	0.012	0.02	ILL	0.46	0.12	0.220	0.06
PROF	0.37	−0.25	0.013	0.04	ELEV	0.54	−0.32	−0.064	0.50	PLAN	0.45	0.10	0.228	0.02
PLAN	0.49	0.15	0.179	0.10	EDAF	0.38	0.09	0.037	0.33	EDAF	0.44	0.10	0.311	0.04
ASPECT	0.25	−0.13	0.451	0.04	TPI	0.29	−0.03	0.191	0.05	ASPECT	0.40	0.06	0.233	0.03
TPI	0.38	−0.09	0.368	0.03	PROF	0.29	−0.03	0.149	0.04	PROF	0.40	−0.03	0.190	0.02
GEOM	0.25	−0.02	0.276	0.00	PLAN	0.30	−0.01	0.193	0.03	TPI	0.41	0.01	0.214	0.01

(D) Debris flows					(E) Flow slides				
FACTOR	*R*	G-K	ARPA	SHIFT	FACTOR	*R*	G-K	ARPA	SHIFT
LITH	0.54	−0.92	0.327	0.05	ROUGH	0.55	0.83	0.384	−0.05
SLOPE	0.45	0.90	0.368	0.03	GEOM	0.49	0.83	0.256	0.07
ROUGH	0.45	0.90	0.417	−0.02	SLOPE	0.42	0.81	0.494	−0.15
TPI	0.43	0.89	0.345	0.03	TWI	0.41	−0.80	0.371	0.08
USE	0.43	−0.67	0.343	−0.10	USE	0.28	−0.60	0.401	−0.15
TWI	0.23	−0.46	0.450	−0.10	LITH	0.26	−0.55	0.450	−0.10
SPI	0.22	0.40	0.168	0.03	SPI	0.03	0.46	0.150	0.04
ELEV	0.34	−0.28	0.334	0.02	ILL	0.34	0.27	0.172	0.10
GEOM	0.34	0.09	0.397	0.01	ASPECT	0.23	0.24	0.292	0.06
DIST	0.06	0.05	0.005	0.02	PLAN	0.33	0.13	0.267	0.05
ASPECT	0.21	0.03	0.238	0.05	TPI	0.31	0.13	0.251	0.03
ILL	0.38	0.03	0.134	0.09	PROF	0.30	0.11	0.232	0.04
PLAN	0.36	0.03	0.334	0.06	DIST	0.10	−0.10	−0.153	0.22
EDAF	0.26	−0.02	0.249	0.02	ELEV	0.30	0.09	0.268	0.03
PROF	0.32	0.00	0.273	0.03	EDAF	0.26	−0.04	0.083	0.14

ASPECT: Aspect (sessagesimal degrees clockwise from N); DIST: Distance of tectonic lineaments (m); EDAF: Edafic units; ELEV: Elevation (m a.s.l.); GEOM: Geomorphological units; ILL: Illumination LITH: Lithology; PLAN: Plan Curvature (rad^{-1}); PROF: Profile curvature (rad^{-1}); SLOPE: Slope angle (sessagesimal dregrees); TWI: Topographic Wetness Index (m); ROUGH: Roughness; TPI: Topographic Position Index; SPI: Stream Power Index; USE: Land use.
R: linear and contingency correlation coefficient; G-K: Goodman and Kruskal's gamma; ARPA: areas above randomly predicted area; SHIFT: shift between prediction and success rate curves.

2.4 Factor selection

Slope stability is directly connected to the types of terrain, to the presence of discontinuity surfaces, to the morphology of the slopes (slope angle, aspect, curvature, land use and hydrogeological conditions, etc.), while the triggering of new landslides, is usually connected to internal and external conditions, such as intensive rainfall or earthquakes. The triggering factors can also be anthropologically induced by deforestation, intensive erosion different uses of lands, drilling, etc. (Crozier, 1984; Hansen, 1984). Landslide susceptibility assessment is based on conditioning factors, as it produces prediction images which depict the spatial distribution of the landslide propensity without allowing for the estimate magnitude or time recurrence for the predicted phenomena. As the aim of this research was to test a variable selection procedure, the factors taken into consideration were those where data and maps were available for processing.

The following 15 controlling factors or variables were considered (Table 2):

Topographic factors: in describing and quantifying the environmental conditions, DEM is the most important data source as it directly influences the quality of the derived factors, (Burrough, 1986). The DEM here used was derived by digitalizing the cartography (1:10 000) made by the Government of Andalusia, which was obtained from aerial photos in scale 1:20 000. The following derived variables were tested for preparing the susceptibility models. Slope aspect (ASPECT), which was reclassified in classes of 45°, from 0 (due north) to 360, (again due north, coming full circle) clockwise. Flat areas, having no downslope direction are given a value of −1. Slope aspect can be considered as a

proxy variable for the attitude of the outcropping layered rocks. Elevation (ELEV), which was reclassified in equal classes from 650 m to 1659 m a.s.l. (Fernández et al., 2008), can express both topographic condition and, indirectly, the role of thermo-pluviometric conditions. Illumination (ILL), ranging from 0 to 255, where 0 represents the shadowed areas and 255 the brightest, allows for the differentiation of cells with respect to evapo-transpiration. Plan curvature (PLAN) (Ohlmacher, 2007) and profile curvature (Dikau, 1989) were reclassified in ½ standard deviation, from −17.2 to +16.4 rad^{-1} and from −16.5 to +22.9 rad^{-1}, respectively. Topographic curvatures control the way in which both surface runoff and gravitative stresses acting on shallow failure surfaces can converge or diverge. Slope angle (SLOPE) was classified in 6 natural break intervals expressed in sessagesimal dregrees – (1) 0°–2°; (2) 2°–5°; (3) 5°–15°; (4) 15°–25°; (5) 25°–35°; (6) >35°. SLO is typically considered the main controlling factor in landslide modelling. Topographic wetness index (TWI), which was reclassified in standard deviation from 4.7 m to 17.9 m (Rodhe and Seibert, 1999; Zinko et al., 2005), expresses a potential index of saturation of soils (Sharma, 2010). Topographic roughness (ROUGH) is a measure of the texture of a surface and was reclassified in 5 classes, from 1 to 1.9 by natural breaks (Hobson, 1972). It is quantified by the vertical deviations of a real surface from a linear planar shape. Topographic position index (TPI) compares the elevation of each cell in a DEM to the mean elevation of a specified neighborhood around that cell (Weiss, 2001; Zinko et al., 2005); it was reclassified in 10 natural break classes from −8.4 to 9.2. TPI allows the expression of the geomorphological setting in a quantitative way. Stream power index (SPI) is the time rate of energy expenditure and has been used as a measure of the erosive power, which can control the initiation of landslides. SPI can be calculated as: SPI = As tan β, where As specific catchment area and tan β is local slope (Sharma, 2010).

Geological l.s. factors: these are derived from available maps which have been validated and detailed for this research through field checks. Lithology (LITO): is one of the most important factors because of its influence on the geo-mechanical characteristics of terrains. The various litho-stratigraphic units outcropping in the area were grouped in 6 lithological classes – (1) Alluvial; (2) Calcarenites, sands, marls and limestones; (3) Calcareous marble; (4) Conglomerates, sands and limestone; (5) Phyllite, micaschist, sandstone; (6) Sand, silt, clay, gravel) – which were defined on the basis of the prevailing rock composition (Clerici et al., 2006). Land use (USE), which was reclassified in six classes: (1) Bush; (2) Permanent crops; (3) Shrubland; (4) Urban areas; (5) Extractive areas; (6) River beds. Distance of tectonic lineament (DIST), which was reclassified in 3 classes: 1 (0–200 m), 2 (200–400 m), 3 (>400 m), corresponding to the distance from the faults and thrust faults. Geomorphological units (GEOM), reclassified in: (1) karst platform; (2) Floodplain. (3) Hills; (4) Mountain chain. Edafic units (EDAF), reclassified in five classes: (1) Calcareous cambisol; (2) Regosol; (3) Lithosol; (4) Luvisol; (5) Fluvisol.

To maximize the resolution of the topographic factors, which were derived from a 1:10 000 map, the pixel size of all square grid layers was set to 10 m, even if the scales of the source maps from which the geological l.s. factors were smaller: land use (1:25 000), lithology, geomorphology and edafic units (1:50 000), DEM (1:10 000).

Before combining the variables in a UCU layer, univariate geostatistical relationships between each variable and landslide were estimated, by analysing the association coefficients of contingency tables. By cross-tabulating a factor grid layer and a landslide vector layer, it is in fact possible to derive contingency tables whose statistical correlation can be quantitatively estimated (Irigaray, 1999; Fernàndez, 1996; Chacón, 2003; Fernàndez, 2003; Irigaray et al., 2007). By using statistical software packages like Unistat and IBM SPSS, the following correlation indexes were computed: linear and contingency correlation coefficient (R), Goodman-Kruskal's gamma (G-K) (Goodman and Kruskal, 1954; Davis, 1973).

The predictive role of each single variable concerning the assessment procedure was also estimated, by validating susceptibility models based on a single factor. The method requires (Chung and Fabbri, 2003) the spatial random partition of the landslide inventory in a training subset, which is exploited to classify the susceptibility levels of the UCUs so to produce a prediction image, and a test subset, which is considered as the unknown target pattern. The prediction image is then compared to the actual spatial distribution of the test rupture zones and success and prediction rate curves are produced. On the contrary, in the only case of translational slide present in the study area where it is not possible to split the diagnostic areas archive (we have just one case), the approach is based on the random division of the (UCU), identifying UCU training and test domains, to obtain the prediction rate curve. Some morphometric indexes of the validation curves were used to estimate the performance of the models. The quality of the susceptibility models was estimated by applying a procedure based on the quantitative analysis of the shape of the success and prediction rate curves, which exploited two morphometric indexes: ARPA, areas above randomly predicted area; and SHIFT, shift between prediction and success rate curves (Rotigliano et al., 2011a, b). Since the diagonal trend attests for a non-effective prediction, a high performance produces high values of ARPA; a good fit of the model is testified by low SHIFT results. By drawing a theoretical validation curve respecting these threshold values, Rotigliano et al. (2011a) indicate 0.12 as the lower limit of ARPA for an effective susceptibility model.

2.5 Models suite

In light of the results of the procedure for evaluating the relevance of each variable, it was possible for each of the

landslide typologies to rank the controlling factors according to a predictivity scale. Authors are aware of the univariate basis of the proposed analysis, so that interaction or confounding effects cannot be determined as factors are then analysed one by one. However, a suite of multivariate models was prepared so to verify if the ranking positions of each factor, which is obtained by applying the above described univariate procedures, are additive or not. Interaction between factors should result in anomalous increasing or decreasing of the prediction skill of models obtained by differently selecting the combined factors from the ranked list.

Among the very high number of possible models which can be prepared for each landslide typology starting from the 15 factors, a representative suite of models is discussed here, which has been defined to the aim of highlighting the way in which the univariate performances of the single variables propagate when the latter are combined in multivariate models. Particularly starting from the single variable best model, predictive performances were estimated both when progressively or randomly adding less performing factors. The results of the multivariate models were submitted to validation by applying both the success and prediction rate curve method and the analysis of the degree of fit (Chung et al., 2003; Chacón et al., 2006; Irigaray et al., 2007; Remondo et al., 2003).

3 Results

3.1 Factors

Table 2a–e shows the results of the analysis of the contingency tables for each landslide typology, showing the factors listed according to a decreasing order of the gamma G-K's absolute value, which was used to indicate the correlation between independent (factors) and dependent (landslides) variables. G-K ranges from -1 to +1: when G-K is close to 1, we have high correlation (for positive values, we have a direct correlation, for negative ones it is indirect or negative); instead, G-K values close to zero indicate no correlation. The predictor variables are classified as "effective" (EFF) or "not effective" (NEF) depending on if the condition G-K index > 0.5 and $R > 0.4$ applies or not (Fernández et al., 1996, 2003; Irigaray et al., 2007).

Slope angle is among the more effective instability factors for all the 5 landslide typologies, having very high G-K values (G-K > 0.8) for falls, debris flows and flow slides. Roughness, land use and topographic wetness index are also among the main causative factors. Roughness has high correlation (G-K > 0.8) for all the typologies, with the exception of earth flow (G-K $= 0.67$) and translational slides, for which it does not enter among the more predictive variables. Land use is a good predictor variable for all the typologies, with the exception of flow slides, while topographic wetness index is not among the effective variables both for debris flows and falls. Among the factors which are classified as EFF variables for only one landslide typology, geomorphologic units, for flow slides, topographic position index and lithology, for debris flows, are strongly (G-K > 0.8) effective. Finally, the distance from tectonic lineaments and illumination, for translational slides and elevation, for earth flows, show medium G-K values. All the other variables do not satisfy the condition and are, in the following, considered as not effective.

By looking at results from the "landslide typology point of view" the following results can be highlighted: falls can be explained by three EFF variable, which produces very high G-K (>0.95) and ARPA (>0.45) values; five EFF variable have been observed for debris flows, giving high G-K (close to 0.9, except for USE) and variably high ARPA values; four variables for flow slides produces G-K values close to 0.8, and medium-high ARPAs; medium G-K and very variably low ARPA values characterise the five explanatory variables for translational slides; the six EFF variable for earth flows, finally, are characterised both by medium G-K and ARPA values.

The relationships between G-K and ARPA can be summarized as follows. The validation of all the univariable models gives high ARPA values, well above the threshold of 0.12 (typically >0.25). Translational slide represents an exception, since the models prepared for SLOPE and DIST do not fit the ARPA threshold limit; for this landslide typology, ARPA values quite above the 0.12 limit are among the NEF variables. Larger (>0.3) ARPA values for NEF single parameter values are observed for falls (EDAF, ELEV, ASPECT, TPI, GEOM), earth flows (GEOM, EDAF), debris flows (TWI, ELEV, GEOM, PLAN) and flow slides (USE, LITH). Five of the latter cases are represented by factors just below the limit of the EFF factors (EDAF, for falls, GEOM, for earth flows, TWI, for debris flows, USE and LITH, for flow slides). ARPA values close or larger than 0.4, seems to be strictly related with EFF variable or, in case of NEFs, with G-K greater than 0.45, with very surprising exceptions of GEOM, for falls and debris flows.

3.2 Multivariate models

According to the results of the contingency tables, for each landslide typology, the factors have been ranked from I (the best predictor) to XV (the least predictor), depending on the value of the association indexes (Table 3). In order to verify both the correctness of the threshold values adopted in classifying the factors and the extent to which univariate correlation between each single factor and landslides propagates onto the predictive performances of multivariate models, a large set of combinations of variables has been used to prepare susceptibility models. The factors have been combined to produce a suite of UCU layers, which have then been intersected with the landslide (rupture zone) archive, to derive the susceptibility grid layer. All the prepared models have been submitted to validation procedures. Particularly *prediction*

Table 3. Summary of classification of the determining factors for each type of slope failure. FLL: falls; TSL: Translation slides; EFL: Earth flows; DFL: Debris flows; FSL: Flow slides.

SUMMARY					
FACTOR	FLL	TSL	EFL	DFL	FLS
ELEV	VIII	XI	VIII	VIII	XIV
SLOPE	**III**	**V**	**VI**	**II**	**III**
ASPECT	XIII	IX	XIII	XI	IX
TWI	VI	**II**	**V**	**I**	**IV**
PROF	XI	XIV	XIV	XV	XII
PLAN	XII	XV	XI	XIII	X
ROUGH	**I**	VII	**IV**	**III**	**I**
TPI	XIV	XIII	XV	IX	XI
SPI	V	X	VII	VII	VII
LITH	VII	**I**	**III**	VI	VI
USE	XV	**III**	**I**	**V**	V
DIST	IX	**IV**	IX	X	XIII
GEOM	**II**	VI	**II**	**IV**	**II**
EDAF	IV	XII	XII	XIV	XV
ILL	X	VIII	X	XII	VIII

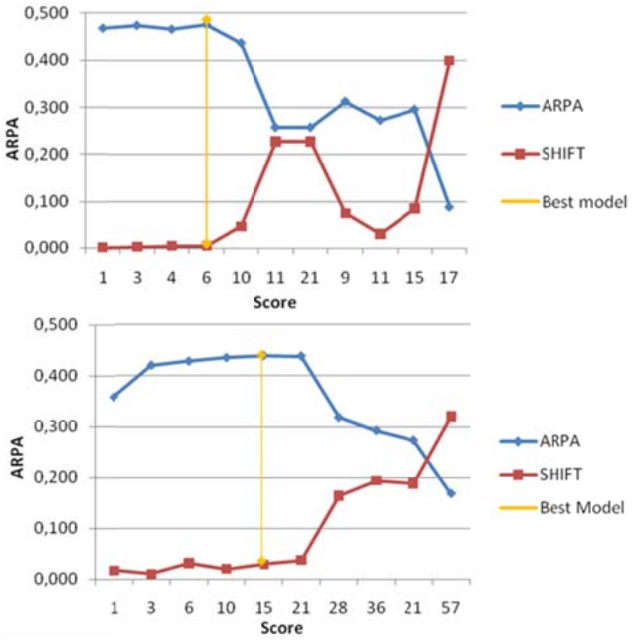

Fig. 5. Correlation between ARPA and SHIFT morphometric indexes for suite models; Falls **(a)**; Debris flows **(b)**.

and *success rate curves* were drawn, by randomly splitting the landslide archive in a *training* and a *test* balanced subsets. For the quantitative evaluation of the results of the validation, two morphometric parameters have been computed (ARPA and SHIFT). Among the great number of models which have been evaluated, the results for the most diffused landslide typologies (falls and debris flows), are discussed (Figs. 5 and 6; Table 4a and b). The two suites of models allowed the verifying of a strong coherence between progressively adding variables to the multivariate models and variation of ARPA. An expected score was computed for each model by adding the rankings of the combined variables (so that the lower the score the more effective the factors). When EFF variables are added to the model, a quite large increasing ARPA and very small stable SHIFT are observed; the maximum ARPA value found for the best model (which includes only EFF variable). A transition to models including NEF variables is clearly marked by best+1 models, prepared by adding to the best models the best of the NEF variables. If another NEF variable is added or a lower score is produced, the decreasing of ARPA is very marked (46 %, for debris flows, 27 % for falls) and strictly coherent with the increasing of SHIFT. For models including also NEF variables, it is possible to observe a clear inverse correlation between ARPA and SHIFT.

In light of the above described results, models for two UCU layers have been prepared for each landslide typologies: best models, including only EFF variables, and best+1 models, which also get the best among the NEF variables. Table 5 lists the results of the validation of the suite of susceptibility models which were prepared, whose validation graphs are shown in Fig. 6. All the models are largely satisfactory, with ARPA values higher than 0.35 and very limited SHIFT (<0.05), with the exception of EFLBEST+1, which is characterised by low ARPA and high SHIFT, and FSLBEST+1, which associate high ARPA to a very high SHIFT. Generally, the best models gave ARPA values greater than the ones which were produced by one of the single combined variables or, when ARPA are similar to the ones resulted from a single factor model (e.g., debris flow and flow slides) a lowering of SHIFT is produced by combining EFF variables. Particularly, the susceptibility models for falls and debris flows, which are prepared by combining EFF variables characterised by high G-K and ARPA (Table 3a and d), confirmed to have a high predictive skill; coherently, the earth flow best model shows a quite (ARPA < 0.4) predictive skill, in accordance to the quite good performances of the single combined variables. Surprisingly, flow slides and translational slides best models produce results opposite to the expected ones. TSLBEST is in fact characterised by very high performance, in spite of the medium to low G-K and ARPA values (Table 2b); on the contrary, FSLBEST gives a results that is similar to the performance of the single combined factors (Table 2e). It seems that variables add in a congruent increasing and incongruent decreasing way, for translational slides and flow slide, respectively. Finally, with regard to the best+1 models, it must be noticed that high ARPA (>0.4) best models are less susceptible to decrease their performance when the best NEF variables are added. For if it were to prove correct, then the consequences would be enormous to say the least.

Table 4. The two suites of models allowed high coherence between the progressive addition of variables to the multivariate models and variation of ARPA; falls (a); debris flows (b).

Model suite: Falls					
MODEL	RANKS	SCORE	COMBINED FACTORS	ARPA	SHIFT
FLL_A	I	1	ROUGH	0.467	0.00
FLL_B	I–II	3	ROUGH-USE	0.474	0.00
FLL_D	I–III	4	ROUGH-SLOPE	0.466	0.01
FLLBEST	I-II-III	6	ROUGH-USE-SLOPE	0.476	0.01
FLLBEST+1	I-II-III-IV	10	ROUGH-USE-SLOPE-EDAF	0.437	0.05
FLL_C	I-II-III-V	11	ROUGH-USE-SLOPE-SPI	0.258	0.23
FLL_G	I-II-III-XV	21	ROUGH-USE-SLO-GEOM	0.258	0.23
FLL_E	IV–V	9	EDAF-SPI	0.313	0.08
FLL_F	V–VI	11	SPI-TWI	0.273	0.03
FLL_H	IV-V-VI	15	EDAF-SPI-TWI	0.296	0.09
FLL_I	IV-VI-VII	17	EDAF-SPI-LITH	0.088	0.40
Model suite: Debris flows					
MODEL	RANKS	SCORE	COMBINED FACTORS	ARPA	SHIFT
DFL_I	I	1	LITH	0.327	0.02
DFL_II	I–II	3	LITH-SLOPE	0.419	0.01
DFL_III	I-II-III	6	LITH-SLOPE-ROUGH	0.427	0.03
DFL_IV	I-II-III-IV	10	LITH-SLOPE-ROUGH-TPI	0.434	0.02
DFLBEST	I-II-III-IV-V	15	LITH-SLOPE-ROUGH-TPI-USE	0.438	0.03
DFLBEST+1	I-II-III-IV-V-VI	21	LITH-SLOPE-ROUGH-TPI-USE-TWI	0.437	0.04
DFLBEST+2	I-II-III-IV-V-VI-VII	28	LITH-SLOPE-ROUGH-TPI-USE-TWI-SPI	0.317	0.16
DFLBEST+3	I-II-III-IV-V-VI-VII-VIII	36	LITH-SLOPE-ROUGH-TPI-USE-TWI-SPI-ELEV	0.292	0.19
DFL_III+XV	I-II-III-XV	21	LITH-SLOPE-ROUGH-PROF	0.273	0.19
DFLBEST+WORST	I-II-III-IV-V-XIII-XIV-XV	57	LITH-SLOPE-ROUGH-TPI-USE-PLAN-EDAF-PROF	0.168	0.32

Table 5. Summary of the results of the validation of the suite of susceptibility models, for best and best+1. FLL: falls; TSL: Translation slides; EFL: Earth flows; DFL: Debris flows; FSL: Flow slides.

MODEL	CODE	COMBINED FATORS	ARPA	SHIFT
FALLS_BEST	FLLBEST	ROUGH-USE-SLOPE	0.476	0.00
FALLS_BEST+1	FLLBEST+1	BESTS+EDAF	0.437	0.05
TRANSLATIONAL SLIDES_BEST	TSLBEST	LITH-TWI-USE-DIST-SLOPE	0.468	0.01
TRANSLATIONAL SLIDES_BEST+1	TSLBEST+1	BESTS+GEOM	0.432	0.05
EARTH FLOWS_BEST	EFLBEST	USE-GEOM-LITH-ROUGH-TWI-SLOPE	0.392	0.00
EARTH FLOWS_BEST+1	EFLBEST+1	BESTS+SPI	0.299	0.11
DEBRIS FLOWS_BEST	DFLBEST	TWI-SLOPE-ROUGH-GEOM-USE	0.438	0.03
DEBRIS FLOWS_BEST+1	DFLBEST+1	BESTS+LITH	0.437	0.04
FLOW SLIDES_BEST	FSLBEST	ROUGH-GEOM-SLOPE-TWI	0.379	0.04
FLOW SLIDES_BEST+1	FSLBEST+1	BESTS+USE	0.334	0.21

3.3 Susceptibility maps and validation

Susceptibility maps for the five best models were prepared, in which six classes, based on a standard deviation reclassification method (from −1 standard deviations to more than 4, with respect a mean value of 9.8 % of density) were used. Adopting standard deviation criteria in depicting landslide susceptibility is coherent with the relative meaning of the concept of susceptibility itself: how much more likely is a new failure in a site with respect to another. The relative error between intersected target landslides by the different susceptibility classes was used to estimate the predictive skill of the maps. The degree of fit was computed for each susceptibility class confirming a very good predictive performance of the five susceptibility models. Finally, a general landslide susceptibility map was produced by cumulating, for each of the

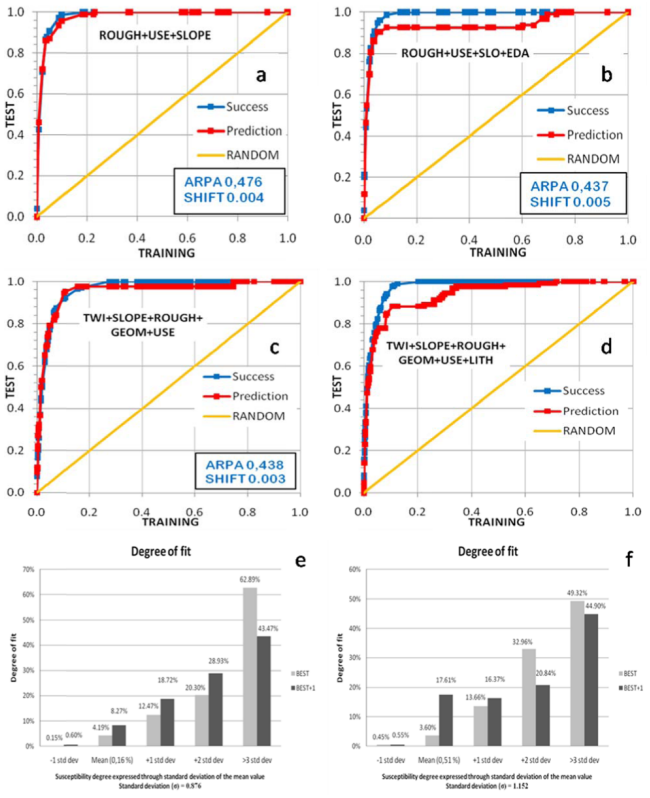

Fig. 6. Comparison of best and best +1 model. With validation curves fall best model **(a)**; fall best+1 model **(b)**; debris flows best model **(c)**; debris flows best+1 model **(d)**. Degree of fit between susceptibility range and falls **(e)** or debris flows **(f)**.

five classes, the landslide area produced for the five typologies. Also in this case, fully satisfactory predictive results have been obtained (Fig. 7a and b).

4 Discussion and concluding remarks

A procedure to select the best determining factors connected to landslide susceptibility has been defined. The method allows the determining factors to be ranked according to their expected contribution to the predictive skill of multivariable model, classifying them as "effective" or "non-effective" and the factors were ranked from I (the best predictor) to XV (the poorest predictor), depending on the value of the association indexes for each landslide typology and establish their best susceptibility model. The identification of the most determinant factors is an important step in a classification process. Statistical methods should be able to get the most parsimonious and geologically meaningful models. The exclusion of poorly related predictive variables is an advantage during the model building procedure allowing to reduce the complexity of the susceptibility model, which in turns become easier to be interpreted from a geological point of view.

Theoretically, a manual selection of the most relevant factors by an expert geomorphologist could be considered the best approach, but because the number of probable descriptors is often large, it is not always actually possible without imposing subjective choice in the model building process. Therefore, the best variables must be selected automatically. The automatic process can be used as a preliminary approach in order to filter unnecessary attributes.

Procedures of forward selection of variables have been applied for logistic regression and discriminant analysis models (e.g., Carrara et al., 2008; Van den Eckhaut et al., 2009). In the present paper, a similar approach is proposed for models based on conditional analysis, which is applicable to the matrix method and unique condition units method. This methodology has been applied to the Beiro River basin in the northeastern area of the city of Granada (Spain).

The results demonstrated that slope angle is among the more effective instability factors for all the 5 landslide typologies studied. Roughness, land use and topographic wetness index are also among the main causative factors. Roughness has high correlation in all the typologies, with the exception of earth flow, for which it is not among the predictive variables. Land use is a good predictor variable for all the typologies, with the exception of flow slides, while topographic wetness index is not among the effective variables for debris flows or falls. The lithology is not always present in the suite of the best models selected by the chosen statistical coefficients. The latter, in fact, is particularly determining for medium-large landslides, for instance earth flows, while is not of great significance for smaller landslides like falls and debris flows. This can be explained by considering that these movements equally affect the debris landslides and those over-consolidated terrains that outcrop in the area, leading to a non-significant statistic in the determining factors. Also, the geological map which was exploited does not have the necessary resolution to produce measurable spatial variations of the terrains with the same detail than the landslide archive does; the lithological terms that we had to adopt do not respond to geo-mechanical properties, as different types of rocks were grouped in single classes. Generally, (earth- and debris-) flow landslides are controlled by topographic conditions together with land use and outcropping lithology, while flow slides are completely explained by topographic continuous (slope, topographic wetness index and roughness) and nominal (geomorphologic unit) features. Topographic wetness index is an important predictor for earth flows and the first among the non-effective for debris flows. Falls are very effectively explained by just two topographic (slope and roughness) and one nominal (land use) attributes. Results for translational slides are heavily affected by the circumstance that just one case was observed.

Generally, the univariable validation method resulted in being coherent with simple association and co-graduation index. At the same time the score (or order of importance) for each variable, which was evaluated on a univariable basis,

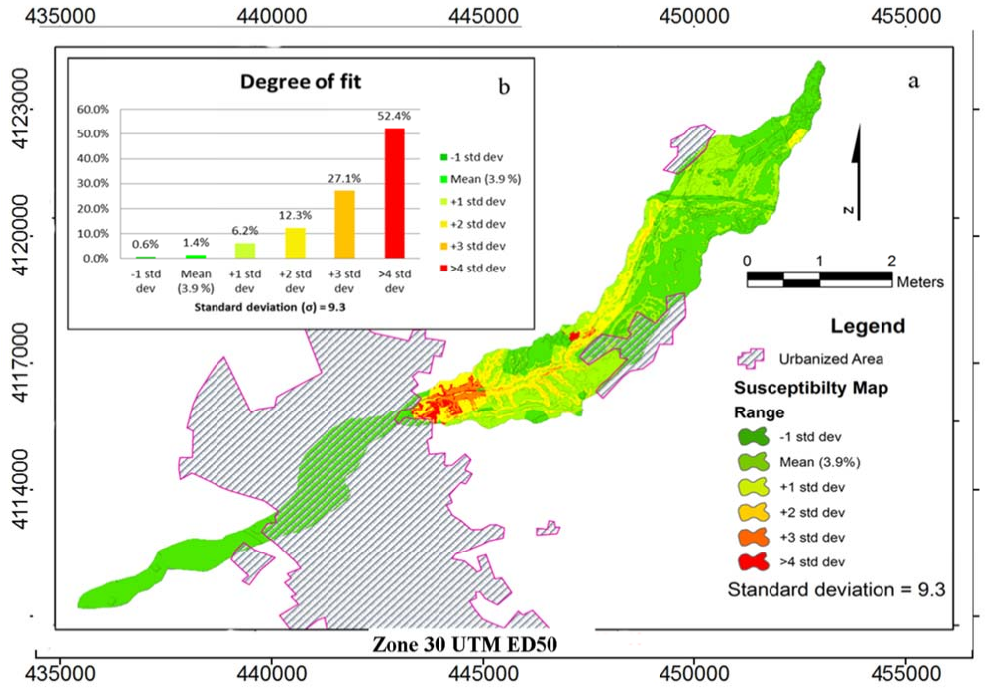

Fig. 7. Landslide susceptibility map **(a)** and validation **(b)**. Coordinate Reference System: UTM zone 30 European Datum 50.

resulted in being coherent with the influence in the performance of the multivariable models: adding an effective variable always resulted in an increasing of the model fitting.

However, the best susceptibility maps obtained following the GIS matrix method and the proposed procedure effectively explain the spatial distribution of slope movements. These maps provide valuable information on the stability conditions of broad regions and are essential in the planning phase to ensure that suitable corrective measures are taken. The option of organizing the controlling factors according to a statistical correlational coefficient could save both economical and time resources. This kind of statistical approach, however, requires excellent quality of the data input, regarding both the variables examined and the details and the resolution of the landslide archive, even though Google Earth™, was of excellent help in identifying the area subject to geomorphological instabilities. The main limit is, thus, due to the scale of the maps available for an area, which is also the scale that the definitive map will have. The possibility of exploiting Google Earth™ images, was here demonstrated on the basis of a comparison of coeval remote and field derived landslide dataset. This tool offers the opportunity to efficiently and more rapidly implement multitemporal landslide archives, allowing us to assess the landslide susceptibility conditions on a regional scale, for very large areas (hundreds of square kilometres) for which landslide archives are typically lacking.

Acknowledgements. The findings and discussion of this research were carried out in accordance with the bilateral agreements between University of Palermo and University of Granada supporting an international PhD programme. Authors have all commonly shared all the parts of the paper. This research was supported by project CGL2008-04854 funded by the Ministry of Science and Education of Spain and was developed in the RNM121 Research Group funded by the Andalusian Research Plan.

Edited by: O. Katz
Reviewed by: S. Leschka and another anonymous referee

References

Burrough, P. A.: Principles of geographical information systems for land resource assessment, Clarendon Press, Oxford, UK, 194 pp., 1986.

Carrara, A., Cardinali, M., Detti, R., Guzzetti, F., Pasqui, V., and Reichenbach, P.: GIS techniques and statistical models in evaluating landslide hazard, Earth Surf. Proc. Land., 16, 427–445, 1991.

Carrara, A., Cardinali, M., and Guzzetti, F.: GIS technology in mapping landslide hazard, in: Geographical Information Systems in Assessing Nat. Hazards., edited by: Carrara, A. and Guzzetti, F., Kluwer Academic Publisher, Dordrecht, The Netherlands, 135–175, 1995.

Carrara, A., Crosta, G., and Frattini, P.: Comparing models of debris-flow susceptibility in the alpine environment, Geomorphology, 94, 353–378, 2008.

Chacón, J.: Los conceptos actuales de susceptibilidad, peligrosidad y riesgo, en la prevención de movimientos de ladera, con ejem-

plos de aplicaciones prácticas, in: 44° Congresso Brasileiro de Geología, edited by: Lima, R. E. and Leite, J. C., Publicaçao Especial, 30 Octubre 2008, "Desastres e riscos geológicos em Curitiba e litoral, Roteiro de Excursao Técnica, CENACID, Curitiba, UFP, 43 pp., 2008a.

Chacón, J.: Movimientos de Ladera. In Master oficial Ingeniería Geológica Aplicada a la Obra Civil, Copicentro, ETS Ingenieros de Caminos, Canales y Puertos, 77 pp., 2008b.

Chacón, J.: Riesgos Geológicos en la Cordillera Bética, in: Geoevents, Geological Heritage and the Role of the IGCP, Lamolda, M. A. (coord.), edited by: Díaz, E., Jiménez Moreno, F., Maurrasse, J-M. R., Meléndez, G., Christopher, R. P., and Rodríguez Tóvar, F. J., Caravaca de la Cruz (Murcia) 15th–18th September 2010, 288 pp., Open Lectures, 255–268, 2010.

Chacón, J. and Corominas, J.: Special Issue on "Landslides and GIS", Nat. Hazards, 30, 263–512, 2003.

Chacón, J., Irigaray, C., Fernàndez, T., and El Hamdouni, R.: Engineering geology maps: landslides and Geographical Information Systems (GIS), Bull. Eng. Geol. Environ., 65, 341–411, doi:10.1007/s10064-006-0064-z, 2006.

Chacón, J., Irigaray, C., EL Hamdouni, R., and Jiménez-Perálvarez, J. D.: Diachroneity of landslides, in: Geologically Active, edited by: Williams, A. L., Pinches, G. M., Chin, C. Y., McMorran, T. J., and Massey, C. I., Taylor and Francis Group, London, ISBN 978-0-415-60034-7, 999–1006, 2010.

Chung, C. F. and Fabbri, A.: Validation of spatial prediction models for landslide hazard mapping. Nat. Hazards 30, pp. 107–142, 2003.

Clerici, A., Perego, S., Tellini, C., and Vescovi, P.: A procedure for landslide susceptibility zonation by the conditional analysis method, Geomorphology, 48, 349–364, 2002.

Clerici, A., Perego, S., Tellini, C., and Vescovi, P.: A GIS automated procedure for landslide susceptibility mapping by the conditional analysis method: the Baganza valley case study (Italian northern Apennines), Environ. Geol., 50, 941–961, 2006.

Conoscenti, C., Di Maggio, C., and Rotigliano, E.: GIS analysis to assess landslide susceptibility in a fluvial basin of NW Sicily (Italy), Geomorphology, 94, 325–339, 2008.

Conoscenti, C., Costanzo D., and Rotigliano E.: Extension of landslide susceptibility models: a test in the platani river basin (southern Sicily). VII Forum Italiano di Scienze della Terra – Geoitalia 2009, September 9–11, Rimini, Italy, Epitome 03.0254, 68 pp., 2009.

Costanzo, D., Cappadonia, C., Conoscenti, C., and Rotigliano E.: Exporting a Google EarthTM aided earth flow susceptibility model: a test in central Sicily, Nat. Hazards, 61, 103–114, doi:10.1007/s11069-011-9870-0, 2011.

Crozier, M. J.: Field assessment of slope instability, in: Slope Instability, edited by: Brunsden, D. and Prior, D. B., Wiley, Chichester, 103–142, Chap. 4, 1984.

Cruden, D. M. and Varnes, D. J.: Landslide types and processes, in: Landslides: Investigation and Mitigation, edited by: Turner, A. and Schuster, L., TRB Special Report, National Academy Press, Washington, 247, 36–75, 1996.

Davis, J. C.: Statistics and data analysis in Geology, Wiley, New York, 1973.

De Martonne, E.: Nouvelle carte mondiale de l'indice d'aridite', Annales de Geographie, 51, 242–250, 1942.

Dikau, R.: The application of a digital relief model to landform analysis in geomorphology, in: Three Dimensional Applications of Geographic Information Systems, edited by: Raper, J., Taylor and Francis, New York, 55–71, 1989.

Dikau, R., Brunsden, D., Schrott, L., and Ibsen M. (Eds.): Landslide recognition. Identification, Movement and Courses. Report No. 1 of the European Commission Environment Programme, Wiley and Sons, Chichester, England, 251 pp., 1996.

Fernández, T., Irigaray, C., El Hamdouni, R., and Chacón, J.: Inventory and analysis of landslides determinant factors in Los Guajares Mountains, Granada (Southern Spain), in: Landslides, Proceeding of the International Symposium on Landslides, edited by: Senneset, K., Balkema, Rotterdam, Vol. 3, 1891–1896, 1996.

Fernández, T., Irigaray, C., El Hamdouni, R., and Chacón, J.: Methodology for landslide susceptibility mapping by means of a GIS. Application to the Contraviesa area (Granada, Spain), Nat. Hazards, 30, 297–308, 2003.

Fernández, T., Irigaray, C., El Hamdouni, R., and Chacón, J.: Correlation between natural slope angle and rock mass strength rating in the Betic Cordillera, Granada, Spain, Bull. Eng. Geol. Environ., 67, 153–164, doi:10.1007/s10064-007-0118-x, 2008.

Goodman, L. A. and Kruskal, W. H.: Measures of association for cross classifications, J. Amer. Statist. Assoc., 49, 123–764, 1954.

Guzzetti, F., Carrara, A., Cardinali, M., and Reichenbach, P.: Landslide hazard evaluation: a review of current techniques and their application in a multi-scale study, Central Italy, Geomorphology, 31, 181–216, 1999.

Guzzetti, F., Reichenbach, P., Ardizzone, F., Cardinali, M., and Galli, M.: Estimating the quality of landslide susceptibility models, Geomorphology, 81, 166–184, 2006.

Hansen, A.: Landslide hazard analysis, in: Slope Instability, edited by: Brunsden, D. and Prior, D. B., Wiley, New York, 523–602, 1984.

Hobson, R. D.: Surface roughness in topography: quantitative approach, in: Spatial analysis in geomorphology, edited by: Chorley, R. J., 225–245, 1972.

Irigaray, C., Fernàndez, T., El Hamdouni, R., and Chacón, J.: Verification of landslide susceptibility mapping: a case study, Earth Surf. Proc. Land., 24, 537–544, 1999.

Irigaray, C., Fernàndez, T., El Hamdouni, R., and Chacòn, J.: Evaluation and validation of landslide-susceptibility maps obtained by a GIS matrix method: examples from the Betic Cordillera (southern Spain), Nat. Hazards, 41, 61–79, 2007.

Jiménez-Pelvárez, J., Irigaray, C., El Hamdouni, R., and Chacón, J.: Building models for automatic landslide-susceptibility analysis, mapping and validation in ArcGIS, Nat. Hazards, 50, 571–590, 2009.

Ohlmacher, G. C.: Plan curvature and landslide probability in regions dominated by earth flows and earth slides, Eng. Geol., 91, 117–134, doi:10.1016/j.enggeo.2007.01.005, 2007.

Remondo, J., Gonzalez, A., Diaz de Teran, J. R., Cendrero, A., Fabbri, A., and Chung, C. J.: Validation of landslide susceptibility maps; examples and applications from a case study in northern Spain, Nat. Hazards, 30, 437–449, 2003.

Rodhe, A. and Seiber, J.: Wetland occurrence in relation to topography: a test of topographic indices as moisture indicators, Agr. Forest Meteorol., 98, 325–340, 1999.

Rotigliano, E., Agnesi, V., Cappadonia, C., and Conoscenti, C.: The role of the diagnostic areas in the assessment of landslide susceptibility models: a test in the Sicilian chain, Nat. Hazards, 58,

981–999, doi:10.1007/s11069-010-9708-1, 2011a.

Rotigliano, E., Cappadonia, C., Conoscenti, C., Costanzo, D., and Agnesi, V.: Slope units based landslide susceptibility model: using validation tests to select controlling factors, Nat. Hazards, 61, 143–153, doi:10.1007/s11069-011-9846-0, 2011b.

Sharma, B.: Simulation of different SPI Models, Int. J. Comput. Appl., 1, 22-25, 2010.

Soeters, R. and van Westen, C. J.: Slope instability recognition, analysis and zonation, in: Landslide investigation and mitigation, edited by: Turner, A. K. and Schuster, R. L., National Research Council, Transportation Research Board Special Report 247, 129–177, 1996.

Van Den Eeckhaut, M., Reichenbach, P., Guzzetti, F., Rossi, M., and Poesen, J.: Combined landslide inventory and susceptibility assessment based on different mapping units: an example from the Flemish Ardennes, Belgium, Nat. Hazards Earth Syst. Sci., 9, 507–521, doi:10.5194/nhess-9-507-2009, 2009.

Varnes, D. J.: Slope movements, type and processes, in: Landslides analysis and control, edited by: Schuster R. L. and Krizek R. J., Washington Transportation Research Board, Special Report 176, National Academy of Sciences, WA, 11–33, 1978.

Vera, J. A.: Geología de España (geology of Spain), SGE-IGME, Madrid 890 pp., 2004.

Weiss, A.: Topographic Position and Landforms Analysis, Poster presentation, ESRI User Conference, San Diego, CA, 2001.

Zinko, U., Seibert, J., Dynesius, M., and Nilsson, C.: Plant species numbers predicted by a topography-based groundwater flow index, Ecosystems, 8, 430–441, 2005.